

Entanglement of mixed macroscopic superpositions: An entangling-power study

M. Paternostro,¹ H. Jeong,² and M. S. Kim¹¹*School of Mathematics and Physics, The Queen's University, Belfast, BT7 1NN, United Kingdom*²*Center for Quantum Computer Technology, Department of Physics, University of Queensland, St. Lucia, Qld 4072, Australia*

(Received 14 October 2005; published 26 January 2006)

We investigate entanglement properties of a recently introduced class of macroscopic quantum superpositions in two-mode mixed states. One of the tools we use in order to infer the entanglement in this non-Gaussian class of states is the power to entangle a qubit system. Our study reveals features which are hidden in a standard approach to entanglement investigation based on the uncertainty principle of the quadrature variables. We briefly describe the experimental setup corresponding to our theoretical scenario and a suitable modification of the protocol which makes our proposal realizable within the current experimental capabilities.

DOI: [10.1103/PhysRevA.73.012338](https://doi.org/10.1103/PhysRevA.73.012338)

PACS number(s): 03.67.Mn, 03.67.Hk, 42.65.-k

I. INTRODUCTION

Entanglement is the key element in many applications of quantum information processing (QIP) ranging from quantum computation [1] to communication [2]. The studies of entanglement represent an active line of research in modern quantum physics which so far has found only partial answers. On the practical side, entanglement is the core of a new *paradigm* for quantum computation [3] and the catalyst for the performance of tasks which are impossible within the classical domain [4].

More recently, the relation between entanglement and thermodynamical properties of macroscopic objects has become the center of an extensive study [5]. The existence of long-range quantum correlations between the parties of a complex many-body system is allegedly the reason for the peculiar behavior of macroscopic properties of solids [6]. In this context, it is intellectually stimulating and pragmatically very important to investigate and understand the existence of entanglement between macroscopic physical systems and the influences of temperature on it [7]. Theoretically, some steps in this direction have been performed with the study of radiation pressure-induced entanglement between a movable mirror and the electromagnetic field of a cavity [8–10].

Very often, the quantitative analysis of even simplified models of interaction faces important practical difficulties related to the necessity of treating non-Gaussian states of continuous-variable (CV) systems. For non-Gaussian states, there is a lack of objective criteria to determine whether or not entanglement is present. In these years, there have been a few proposals designed to bypass this problem, including Refs. [11,12]. Unfortunately, so far a totally satisfactory answer has not been provided. This serious limitation largely affects the extent to which an analysis of thermally entangled systems can be conducted. A way to bypass the problem is given by the formal restriction of the Hilbert space of the composite CV system to an effective discrete one [13,14], where necessary and sufficient conditions for the existence of bipartite entanglement can be used [15]. However, even though this strategy is theoretically exploitable, its experimental realization is extremely hard.

In this paper, we investigate the entanglement properties of a class of states which have been very recently introduced

by Jeong and Ralph [16] in order to provide a reasonable analogy of the macroscopic quantum superposition (Schrödinger's cat) paradox [17]. The entangled state in Ref. [16] can be considered as a generalization of the two-mode Schrödinger catlike state [18], which corresponds to an entangled state between microscopic and macroscopic systems, to a thermal mixture. The macroscopic part of this catlike state is represented by the displaced thermal state of a harmonic oscillator while the microscopic part is an atomic (or single photon) qubit. The other type of entangled state studied in Ref. [16] corresponds to an entangled state between two macroscopic systems and can be generated through an additional conditional measurement. Such a state can be understood as a generalization of an entangled coherent state [19], which has been found useful for QIP [20], to a thermal mixture. For the second type of the macroscopic entangled state, it was found that Bell's inequality can be violated up to the maximum bound even though the thermal temperature becomes extremely large [16]. On the other hand, the existence and degree of entanglement in the first type of microscopic-macroscopic entangled state, which we shall call "generalized catlike state," remains a question to be answered. In other words, the first question that should be answered in this paper is "how much entanglement can be generated by an interaction between microscopic quantum state (qubit) and macroscopic classical system (thermal state) without any additional process when the temperature becomes large?"

Unfortunately, the states which we are interested in are non-Gaussian mixed CV states for which the known entanglement criteria for CV states [21] fail, leaving a degree of ambiguity which prevents any firm statement on the presence of quantum correlations. To bypass this problem, we describe an alternative theoretical method which is then corroborated by testing the entangling power of the generalized catlike state [22]. The test is based on the capability of a state to induce entanglement, by means of only bilocal interactions, between two initially uncorrelated qubits. As local unitary operations alone cannot create entanglement, the entangling power provides a sufficient condition for the inseparability of the CV state being investigated and, quantitatively, a lower bound to the entanglement originally present in the CV state. Therefore, another question that we

naturally address in this paper is “how can we transfer the entanglement generated by a microscopic-macroscopic interaction to the initially separable bipartite system of two non-interacting qubits?”

Differently from the above mentioned effective-projection technique [10,13], our procedure is operative as it is immediate to design the general scenario for an experimental investigation. This approach can be extended to other non-trivial classes of non-Gaussian CV states, for example, the states which can be generated from the generalized catlike state by measuring the microscopic part of the superposition and subsequently unitarily manipulating the remaining macroscopic part. This results in the coherent superposition of thermally averaged two-mode states. Again, the application of the entangling power test shows the ability to induce entanglement in a two-qubit system. Our analysis reinforces the ideas related to the possibility of macroscopic entanglement at nonzero temperature. We thus provide a tool in the non-trivial problem of the quantitative analysis of the properties of non-Gaussian states which is flexible enough to reveal temperature-resilient macroscopic entanglement.

The remainder of this paper is organized as follows. In Sec. II, we introduce a generalized catlike state, which is a macroscopic nonlocal state. We first address the behavior of the state’s variance matrix to show that the Simon’s CV-state entanglement criterion fails in revealing any quantum correlation in this state. On the other hand, by changing picture and restricting the attention to bidimensional subsectors of the infinite dimensional Hilbert space of the CV subsystem, it is possible to infer the entanglement properties of this class of generalized catlike states. This approach allows us to highlight the striking effects of temperature and displacement (in the phase space) over the entanglement of the state, thus providing an important quantitative insight into its properties. In Sec. III, by adopting the entangling power viewpoint, we show that entanglement can be reliably transferred to two independent qubits which have interacted with the state under investigation, giving us the possibility of constructing a highly entangled quantum channel of static qubits. On the other hand, this approach provides us with a way to detect entanglement in the CV state simply by looking at the state of two qubits. Section IV describes exactly this experimental protocol and a modified one which, with limited modifications to the original idea, turns out to be realistic. Finally, in Sec. V we resume the central results of our analysis and complement it with a brief study the entanglement of thermally weighted entangled coherent states. We show that the entangling power is an exploitable tool in this case as well and reveals the presence of entanglement within a significant range of temperature.

II. GENERALIZED CATLIKE STATES

Let us consider the interaction of a qubit of its logical states $\{|0\rangle, |1\rangle\}_m$, initially prepared in the balanced linear superposition $|+\rangle_m = (1/\sqrt{2})(|0\rangle + |1\rangle)_m$, with the macroscopic part of the generalized catlike state here represented by a physical system M in an initial displaced thermal state $\rho_M^{\text{th}}(V, d) = \int d^2\alpha P_M^{\text{th}}(V, d) |\alpha\rangle_M \langle\alpha|$ (see Fig. 1). We have intro-

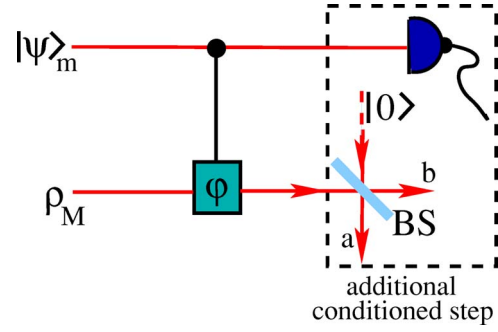


FIG. 1. (Color online) Scheme of principle of the protocol to produce the generalized version of the catlike state (microscopic-macroscopic entangled state) and the second class of thermally weighted entangled coherent states (performed by the additional conditioned step depicted in the dashed box). The conditional- φ gate is the effective evolution induced by the cross-Kerr interaction between the microscopic part m (in the pure state $|\psi\rangle_m$) and the macroscopic one in the thermal displaced state ρ_M^{th} . BS is a 50:50 beam splitter and the symbol for a detector is also shown.

duced the coherent state $|\alpha\rangle$ of its amplitude $\alpha = |\alpha|e^{i\zeta} \in \mathbb{C}$ and the thermal probability distribution

$$P_M^{\text{th}}(V, d) = \frac{2}{\pi(V-1)} e^{-2|\alpha - d|^{2/(V-1)}}, \quad (1)$$

where V is the variance of the distribution, related to the temperature of the thermal distribution by the relation $V = (e^{\beta\omega} + 1)/(e^{\beta\omega} - 1)$ with $\beta^{-1} = k_B T$ ($\hbar = 1$ is assumed throughout the paper). Here, k_B is the Boltzmann constant, T is the radiation temperature, and ω its frequency. We have indicated with d the displacement of the state from the origin of the phase space. The relation between the variance and the mean photon number \bar{n} of the field is $V = 2\bar{n} + 1$. The interaction is ruled by the cross-phase modulation Hamiltonian $\hat{H}_K = \chi \hat{m}^\dagger \hat{m} \hat{M}^\dagger \hat{M}$. Here \hat{m} and \hat{m}^\dagger (\hat{M} and \hat{M}^\dagger) are the annihilation and creation operators of the microscopic (macroscopic) system, respectively, and χ is the rate of nonlinearity of the interaction [16]. After an interaction time t , the dynamical evolution corresponding to the Hamiltonian \hat{H}_K gives rise to the state

$$\rho_{mM}^{\text{ent}} = \int d^2\alpha P_M^{\text{th}}(V, d) |\psi\rangle_{mM} \langle\psi|, \quad (2)$$

with $|\psi\rangle_{mM} = (1/\sqrt{2})(|0, \alpha\rangle + |1, \alpha e^{i\varphi}\rangle)$. Here, $\varphi = \chi t$ is the cross-phase shift induced by the model \hat{H}_K .

In order to pursue our investigation, we find it convenient to preliminarily consider just the pure superposition $|\psi\rangle_{mM}$, whose entanglement properties we want to quantitatively address. This state has been considered as a reasonable example of Schrödinger cat state and has been experimentally produced as an entangled state of internal and external degrees of freedom of a single trapped ion [18]. Clearly, for $\langle\alpha|\alpha e^{i\varphi}\rangle = 0$, this state carries almost one ebit of entanglement. However, the asymmetric non-Gaussian nature of this superposition makes the entanglement analysis of this state quite nontrivial. For instance, the entanglement does not

emerge at the level of the variance matrix. The variance matrix of a two-mode CV state is defined as $V_{\mu\nu} = \langle \{\hat{x}_\mu, \hat{x}_\nu\} \rangle$ ($\mu, \nu=1, 2$). The variance matrix is in one-to-one correspondence with the characteristic functions of a Gaussian CV state which, in turns, gives us information about the actual state of the system [23,24]. However, this is not true for the non-Gaussian state $|\psi\rangle_{mM}$, whose variance matrix reads

$$\gamma_{mM}^{\text{ent}} = \begin{pmatrix} \mathbf{A} & \mathbf{C} \\ \mathbf{C}^T & \mathbf{B} \end{pmatrix}$$

with $\mathbf{A}=2\mathbb{1}$,

$$\mathbf{B} = 2|\alpha|^2 \begin{pmatrix} 1 + \cos \varphi \cos(2s) & \sin(2s)\cos \varphi \\ \sin(2s)\cos \varphi & 1 - \cos \varphi \cos(2s) \end{pmatrix} + \mathbb{1} \quad (3)$$

and

$$\mathbf{C} = \alpha_\varphi \begin{pmatrix} \cos(s)\cos(r) & \sin(s)\cos(r) \\ \cos(s)\sin(r) & \sin(s)\cos(r) \end{pmatrix}. \quad (4)$$

Here we have defined $\alpha_\varphi = 2|\alpha|e^{-|\alpha|^2(1-\cos \varphi)}$, $s = \zeta + \varphi/2$ and $r = |\alpha|^2 \sin \varphi + \varphi/2$. We have found that Simon's separability criterion [21,25] which is the most successful criterion for CV entanglement, is not able to show quantum correlations in this state. Interestingly enough, the criterion fails for $\varphi = \pi$ which is the value at which one would expect the largest degree of entanglement to be found between the subsystems. We have also checked that the conditions for inseparability established in Ref. [12] is not verified by the state we are considering so that other ways have to be researched. The above intuitive expectation about the entanglement at $\varphi = \pi$ is confirmed by the following simple analysis. The state $|\psi\rangle_{mM}$ can be written in its Schmidt decomposition as

$$|\psi\rangle_{mM} = \sqrt{\lambda_-} |\Phi_+\rangle_m |\Psi_+\rangle_M + \sqrt{\lambda_+} |\Phi_-\rangle_m |\Psi_-\rangle_M, \quad (5)$$

where $|\Phi_\pm\rangle_m = (1/\sqrt{2})(|0\rangle \pm e^{2i|\alpha|^2 \sin \varphi} |1\rangle)_m$ and $|\Phi_\pm\rangle_M = N_\pm (|\alpha\rangle \pm e^{-i|\alpha|^2 \sin \varphi} |\alpha e^{i\varphi}\rangle)_M$ with the normalization factors

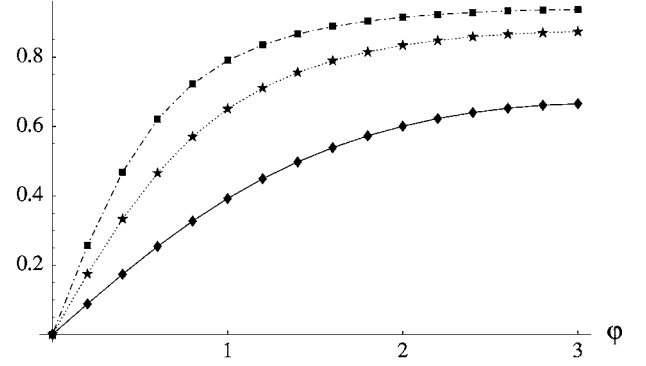
$$N_\pm = \frac{1}{\sqrt{2\{1 \pm \exp[-|\alpha|^2(1 - \cos \varphi)]\}}}. \quad (6)$$

The coefficients of the superposition (5) are defined in terms of the N_\pm factors as $\lambda_\pm = N_\pm^2 / (N_+^2 + N_-^2)$. In order to quantify the entanglement within a state of its density matrix ρ_{ab} , we use the negativity of partial transposition (NPT) [26]. NPT is a necessary and sufficient condition for entanglement of any bipartite qubit state [26]. The corresponding entanglement measure is defined as $\mathcal{E} = \max\{0, -2\epsilon^-\}$ with ϵ^- the negative eigenvalue of the partial transposition of ρ_{ab} with respect to one of its parties. The entanglement in $|\psi\rangle_{mM}$ can be expressed as

$$\mathcal{E}_{\psi_{mM}} = \sqrt{1 - e^{-2|\alpha|^2(1 - \cos \varphi)}}. \quad (7)$$

In the range $\varphi \in [0, \pi]$ and regardless of $|\alpha|$, Eq. (7) is a monotonously increasing function of the phase φ saturating at $\mathcal{E}_{\psi_{mM}}(|\alpha| \gg 1) = 1$. The saturation value of this function depends on $|\alpha|$ and, as a function of the interaction phase φ , is reached faster as $|\alpha|$ is increased. The Schmidt decomposi-

Entanglement



Entanglement

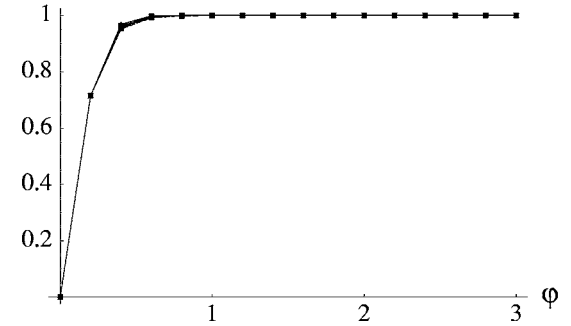


FIG. 2. Entanglement in the generalized catlike state ρ_{mM}^{ent} against the interaction phase φ , for different values of the variance V . In panel (a) we have considered the displacement $d=1$. From bottom to top, the curves show the behavior of the entanglement as V is increased. We have considered $V=2$ (\blacklozenge), $V=5$ (\star), and $V=10$ (\blacksquare). Panel (b) shows the results for $d=7$ showing that, for larger d , the curves relative to different V 's get so close to become indistinguishable. The saturation to one ebit of entanglement is nearly independent of the temperature of the thermal distribution.

tion of $|\psi\rangle_{mM}$ is a useful tool in order to test in a simple way the entanglement present in the thermally weighted superposition ρ_{mM}^{ent} . By applying the NPT criterion, we find that $\mathcal{E}_{\rho_{mM}^{\text{ent}}} = 2 \int d^2 \alpha P_M^{\text{th}}(V, d) \sqrt{\lambda_- \lambda_+}$ which, involving the double Gaussian integration of the square root of an exponential function is, in general, hard to compute analytically. Nevertheless, it has been possible to numerically sample the behavior of this function against the interaction phase φ , for different values of the variance V and the displacement d . The results are shown in Figs. 2(a) and 2(b), where $d=1$ and $d=7$ have been considered, respectively. Evidently, the thermal weighting of the superposition does not smear out the entanglement in the bimodal state. Significant entanglement can be found for any value of the variance V (i.e., at any value of the temperature considered). By looking at Fig. 2(a) we see that, as the variance V increases, more entanglement is found in the state in Eq. (2). This can be understood by considering that a larger V signifies the inclusion of pure component terms $|\psi\rangle_{mM} \langle \psi|$ corresponding to larger values of $|\alpha|$ in the mixed state (2). These pure component states with larger $|\alpha|$ are associated with large degrees of entanglement. Despite the increase of the thermal nature, the increase of the contribution of the pure component states with larger en-

tanglement results in the overall increase of the degree of entanglement $\mathcal{E}_{\rho_{m,M}^{\text{ent}}}$.

Moreover, as soon as a large displacement d is considered, the differences between the results corresponding to distributions characterized by increasing variances becomes irrelevant. The saturation value of entanglement is reached regardless of the actual value of V [see Fig. 2(b)], quicker than the case of a small d . This matches the results found in terms of the negativity of the Wigner function associated with the state ρ_{mM}^{ent} which, for moderate values of V , deepens its negative part for larger values of d .

On the other hand, this effect represents a huge practical advantage in the production of the entangled state we are studying. Indeed, it is well known that the currently achievable rates of nonlinearity are not sufficiently large to guarantee an interaction phase $\varphi = \pi$ [28]. This would signify that, for a small V , the produceable entanglement would be very faint [see Fig. 2(a)]. However, it is sufficient to displace the thermal field more in order to achieve a significant improvement in the rate of entanglement generation. The reason behind such a behavior relies on the increased distinguishability of the components of a pure microscopic-macroscopic superposition achieved for a displacement d from the origin of the phase space. Indeed, if a small φ is available, one way to increase the distinguishability between $|\alpha\rangle$ and $|\alpha e^{i\varphi}\rangle$ is the use of the coherent states having larger amplitudes [29]. This is exactly the mechanism behind the results shown in Fig. 2(b). This strategy is perfectly in line with the idea of using weak nonlinearities for various applications [30,31]. Thus, our scheme seems to be experimentally accessible even in the more realistic situation of a small Kerr nonlinearity.

We believe that this result is important in the context of entanglement in mesoscopic systems at finite temperatures [10,32] as we have shown a model where the quantum nature of a microscopic resource is enough in order to induce intrinsically quantum features in a macroscopic object (as our displaced thermal field). These features, which are temperature resilient, can be highlighted by partitioning the CV Hilbert space into quadruplets at fixed α and averaging over the temperature-dependent probability distribution.

III. TRANSFER OF QUANTUM PROPERTIES TO MICROSCOPIC OBJECTS

In this section we address a relevant question related to the possibility of transferring the quantum correlations established in the generalized catlike state ρ_{mM}^{ent} to the initially separable bipartite system of two noninteracting qubits. This problem is worth addressing under many viewpoints. *In primis*, would the entanglement set in the generalized catlike state be useful if a quantum channel has to be realized? In the context of distributed QIP, this is a relevant question as it has been shown that reliable channels, exhibiting genuine quantum features, are an irremissible resource for the performances of quantum computation [33]. On the other hand, the interface between heterodimensional systems is *per se* a hot topic which has attracted a considerable attention, recently, especially focused onto the transfer of entanglement from a

CV system to one which *lives* in a discrete Hilbert space [22,34]. Finally, while the tomographic reconstruction of the properties of a CV system is a hard task to perform, its discrete-variable counterpart may be accomplished with much easier experimental protocols [35]. It would be thus desirable to design a protocol which allows one to infer the entanglement within a CV state without relying on its direct tomography. In a discrete-variable system this is possible through, for instance, entanglement witnesses detected with a minimal number of measurements [36].

Such a protocol is provided by the research for the entanglement generated in a discrete-variable bipartite subsystem by the CV one via some local qubit-CV interaction. This gives a sufficient criterion for the entanglement between the field modes [22]. Indeed, if the two CV modes are separable, there is no way that, through simple local interactions, quantum correlations could be established. This strategy has been already proven to be efficient in revealing the entanglement between two CV modes which have been fed into two spatially separated cavities and interacted with a pair of qubits. The question of there being any entanglement left between the cavity field modes after the interaction with the qubits has found a positive quantitative answer through the analysis of the entangling power. This is the strategy we would like to use here.

Of course, the quantitative results will depend on the model chosen for the local mode-qubit interaction. However, the implementation of an arbitrary model for light-matter interaction is not a trivial point. Specifically, it is a physical setup-dependent issue (meaning that certain physical setups enable the implementation of certain interaction models more straightforwardly than others). It is the physical system that one has in mind which dictates the most suitable form of the local interaction. Nevertheless, recently it has been shown that the standard Jaynes-Cummings (JC) model for resonant (as well as dispersive) qubit-boson interaction is common to many different physical realizations of a quantum device and in a range of frequency from microwave to optical [27]. This dresses with physical significance the choice of the interaction $\hat{H}_{ij} = \Omega(\hat{a}_i \hat{\sigma}_j^+ + \text{H.c.})$ [(i, j) = (m, a) for the first field mode-qubit system and (i, j) = (M, b) for the second] to govern the local dynamics of each qubit-field mode subsystem. Here, $\hat{\sigma}_j^+ = \hat{\sigma}_j^{-\dagger} = |1\rangle\langle 0|$ is the raising operator of the j th qubit (ordered logical basis $\{|0\rangle, |1\rangle\}$) and Ω is a coupling strength. In the qubit computational basis, this interaction is the generator of the propagator

$$\hat{U}_{ij}(\tau) = e^{-i\hat{H}_{ij}\tau} = \begin{pmatrix} \cos(\tau\sqrt{\hat{a}^\dagger \hat{a}}) & -i\hat{a}^\dagger \frac{\sin(\tau\sqrt{\hat{a}^\dagger \hat{a} + 1})}{\sqrt{\hat{a}^\dagger \hat{a} + 1}} \\ -i\hat{a} \frac{\sin(\tau\sqrt{\hat{a}^\dagger \hat{a}})}{\sqrt{\hat{a}^\dagger \hat{a}}} & \cos(\tau\sqrt{\hat{a}^\dagger \hat{a} + 1}) \end{pmatrix} \quad (8)$$

with $\tau = \Omega t$ being a rescaled interaction time.

It is convenient to proceed with the entangling power test by previously considering the initial separable state $|\psi\rangle_{mM} \otimes |00\rangle_{ab}$ and their joint dynamics $\hat{U}_{ma, Mb} = \hat{U}_{ma} \otimes \hat{U}_{Mb}$.

Tracing out the CV degrees of freedom, we are left with the two-qubit density matrix

$$\begin{aligned} \rho_\psi(\tau) &= \text{Tr}_{mM}[\hat{U}_{ma,Mb}|\psi\rangle_{mM}\langle\psi| \otimes |00\rangle_{ab}\langle 00| \hat{U}_{ma,Mb}^{-1}] \\ &= e^{-|\alpha|^2} \sum_{n=0}^{\infty} \frac{|\alpha|^{2n}}{n!} \begin{pmatrix} A & iG_1 & iG_2 & -G_3 \\ -iG_1 & B_1 & F_1 & iF_2 \\ -iG_2 & F_1 & B_2 & iH_1 \\ -G_3 & -iF_2 & -iH_1 & B_3 \end{pmatrix} \end{aligned} \quad (9)$$

with the explicit expressions for the density matrix elements

$$\begin{aligned} A &= [1 + c_1^2(\tau)]c_n^2(\tau), & G_1 &= \frac{1 + e^{-i\varphi}c_1^2(\tau)}{\sqrt{n+1}}\alpha^*c_n(\tau)s_n(\tau), \\ G_2 &= e^{-i\varphi n}s_0(\tau)c_n^2(\tau), & G_3 &= \frac{e^{-i\varphi(n+1)}s_0(\tau)}{\sqrt{n+1}}\alpha^*s_n(\tau)c_n(\tau), \\ B_1 &= \frac{1 + \cos^2\tau}{n+1}|\alpha|^2s_n^2(\tau), & F_1 &= \frac{e^{-i\varphi n}s_0(\tau)}{\sqrt{n+1}}\alpha c_n(\tau)s_n(\tau), \\ B_2 &= s_0^2(\tau)c_n^2(\tau), & F_2 &= \frac{e^{-i\varphi(n+1)}s_0(\tau)}{n+1}|\alpha|^2s_n^2(\tau), \\ B_3 &= \frac{s_0^2(\tau)}{n+1}|\alpha|^2s_n^2(\tau), & H_1 &= \frac{e^{-i\varphi}s_0^2(\tau)}{\sqrt{n+1}}\alpha^*c_n(\tau)s_n(\tau). \end{aligned} \quad (10)$$

Here we have used the notation $c_n(\tau) = \cos(\tau\sqrt{n})$, $s_n(\tau) = \sin(\tau\sqrt{n+1})$. Equations (10) have now to be integrated over the thermal weighting function in order to gather the reduced density matrix of the qubits after the interaction with ρ_{mM}^{ent} . By exchanging the summation in Eq. (9) and the Gaussian integrals and using the binomial formula, evaluating the integral over $P^{\text{th}}(V, d)$ results in the introduction of the functions

$$\begin{aligned} \Theta_n^j(V) &= \sum_{l=0}^{n+j} \binom{n+j}{l} \left(\frac{V-1}{V+1}\right)^l \Gamma\left(l + \frac{1}{2}\right), \\ \Lambda_n^j(V, d) &= \sum_{l=0}^{2(n-l)+j} \binom{2(n-l)+j}{r} \left(\frac{2d}{V+1}\right)^{2(n-l)-r+j} \\ &\quad \times \left(\frac{V-1}{V+1}\right)^{r/2} \frac{1}{2} [1 + (-1)^r] \Gamma\left(\frac{r+1}{2}\right) \quad (j=0,1,2), \end{aligned} \quad (11)$$

where $\binom{n}{l}$ is the symbol for the binomial coefficient and $\Gamma(r)$ is the Gamma function of its argument r but in a density matrix of the same form of Eq. (9). The explicit eigenvalues of the integrated density matrix are not very informative as their form is quite complicated [37]. Nevertheless, it is possible to evaluate them numerically for a considerable range of V 's and d 's. Some striking results are presented in Fig. 3 for $V=10$ (corresponding to an average photon number $\bar{n}=4.5$) and displacement $d=7$ (\star) and $d=10$ (\blacklozenge). It is evident that the same effect shown in Fig. 2(b), regarding the in-

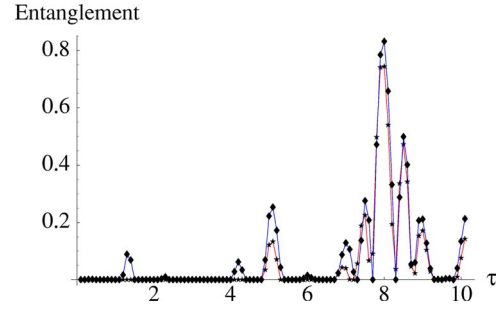


FIG. 3. (Color online) Entangling power of the state $\int d^2P_M^{\text{th}}(V, d)\rho_\psi(\tau)$ for $V=10$ and $d=10$ (\blacklozenge , blue line) and for $V=10$ with $d=7$ (\star , red line). In both the simulation, $\varphi=\pi$ has been assumed. The horizontal axis shows the rescaled interaction time $\tau=\Omega t$.

crease in d , is achieved in the amount of entanglement transferred to the initially separable qubits. It is particularly interesting to stress the considerably large amount of transferred entanglement. In this situation a significantly entangled two-qubit channel can thus be constructed by exploiting the CV entangler represented by ρ_{mM}^{ent} . The usefulness of such a channel has to be quantified by including, in this analysis, the mixedness properties of the two-qubit state. Indeed, it is known that, for instance, a bipartite mixed state becomes useless for quantum teleportation whenever its linearized entropy $S_l = (4/3)[1 - \text{Tr} \rho_{12}^2(r, t)]$ exceeds $2/3$ [38]. S_l is a good measure for mixedness which ranges from 0 (for pure states) to 1 (for maximally mixed ones). The calculation of the linearized entropies corresponding to the examples reported in Fig. 2 and their comparison to the threshold for quantum teleportation is presented in Fig. 4, showing the high-entanglement bumps which corresponds to a sufficiently pure state. The channel, in this case, can be faithfully used for quantum teleportation protocols.

Some remarks are due, in this context. The way the above entangling power test has been constructed immediately makes clear that a quantitative lower bound (even though not a tight one) to the quantum correlations in the CV state is represented by the amount of entanglement found between the qubits. From this point of view, the correct theoretical interpretation of the results shown in Figs. 3 and 5(a) is that the entanglement between modes m and M is, at least, as

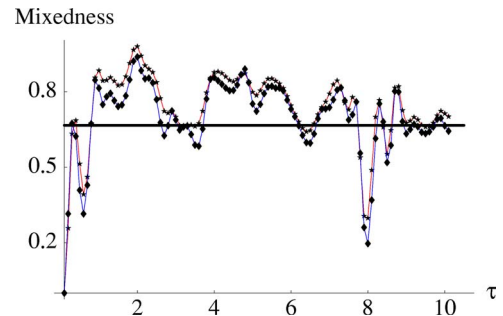


FIG. 4. (Color online) Mixedness of the state $\int d^2P_M^{\text{th}}(V, d)\rho_\psi(\tau)$ against the rescaled interaction time τ for the same parameters as Fig. 3. Also shown the mixedness threshold for a two-qubit state for quantum teleportation (thick straight line).

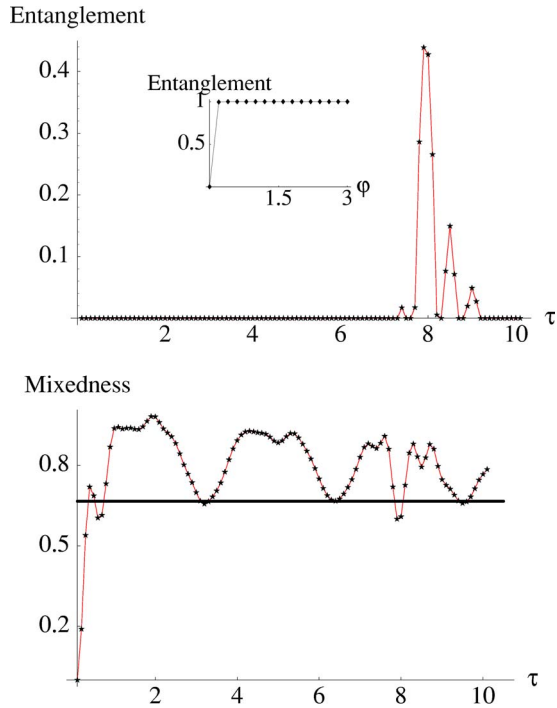


FIG. 5. (Color online) (a) Entangling power of the state $f d^2 P_M^{th}(V, d) \rho_{\psi}(\tau)$ for $V=100$ and $d=20$. The inset shows the entanglement, against ϕ , in the corresponding ρ_{mM}^{ent} . (b) Mixedness of the same state as a function of the rescaled interaction time. The mixedness threshold for teleportation is also shown (straight line).

large as the largest peak shown there. Obviously, this does not allow us to attach a special meaning of good entanglement measure to this peak value (analogous considerations may be done regarding the zones where the transferred entanglement is zero which cannot be straightforwardly interpreted as regions where the two modes are separable). On the other hand, regarding the behavior of the mixedness function, the regions associated to a higher purity of the two-qubit state can be put in correspondence with the optimal transfer of information (quantum correlations) occurred from the two-mode CV state to the qubit one. The entangling power, indeed, is based on a process of entanglement transfer between the two subsystems which occurs at the expense of the intrasubsystem correlations. As time goes by, the quantum nature of the photon number gives rise to a discrete distribution of Rabi frequencies which, in turn, is responsible for the effect of collapses and revivals of entanglement between the qubits [39]. When the entanglement is transferred maximally to the qubits, the entanglement between the qubits and the CV modes is minimized [22]. Thus, at that particular interaction time, the state of the qubits is nearly entirely separable from the state of the CV subsystem. If we start from a pure state for the total system, we know that two subsystems become pure as they are not entangled. However, in our case, the initial state for the total system is mixed. It is therefore interesting to note that even with the mixed property of the initial field, the qubit state becomes quite pure at the time when the qubits and the CV are less entangled. The periodicity of the Rabi floppings, then, reverses the process at later time, thus increasing the mixedness.

It is worth stressing the nonmonotonic behavior of the entangling power against the entanglement initially present in the CV state. This is a well-known feature of this entanglement test [22] and is a result of the interference of the Rabi flopping induced by the distribution of photons characterizing each state having a specific value of V and d . As a specific instance of this peculiar nonlinear relation between the amount of entanglement initially contained in the CV entangler and what is finally found in the two-qubit reduced state, we consider the case of $V=100$ with $d=20$. The analysis conducted in Sec. II results in an entanglement which rapidly approaches 1, as shown in the inset of Fig. 5(a), a behavior quite consistent with the trend shown in Fig. 2(b). On the other hand, the entanglement transferred to the two-qubit state is never larger than 0.45, as evidenced by Fig. 5(a), which is smaller than the entanglement transferred to the qubits for $V=10$, $d=7$. We believe this result is still extremely significant as the high value of V considered here (corresponding to $\bar{n}=49.5$ photons) shows that quite a considerable entangling power is in a high-temperature generalized catlike state. Coming back to the example of teleportation we have addressed, the corresponding two-qubit channel is still useful as its mixedness, at $\tau=8$, can be well below the threshold [see Fig. 5(b)].

IV. PROPOSAL FOR THE EXPERIMENTAL VERIFICATION

In the previous section we have theoretically addressed the question of how to infer the entanglement between the subsystems of a generalized catlike state. On a practical side, however, if our attention is restricted to the case of traveling-wave fields, some problems have to be faced.

In the first place, we have already stressed the difficulties related to the achievement of large-enough rates of nonlinearity. In Sec. II we have outlined a strategy to highlight the quantum correlations in generalized catlike states generated with smaller interaction phases ϕ 's. Nevertheless, the realization of even small ϕ 's would pass, for instance, through the use of long optical fibers where the effect of dephasing channel is still an unknown issue [31].

In the second place, the realization of the entangling power test would require a demanding (even if foreseeable) experimental setup. In Fig. 6 we sketch the scheme of the idea put forward in Sec. III. The generalized catlike state being embodied by two traveling field modes following the general scheme of Fig. 1, would feed two optical cavities, each crossed by a two-level atom (or containing an integrated quantum dot, as an alternative). The passage of the atoms would set each cavity field mode in resonance with the external driving mode, which will penetrate the cavity and interact with the two-level system through the dynamics described in Eq. (8). Each step required by this experimental setup has been independently demonstrated (see Ref. [22], and references within, for a detailed discussion) and we will not comment further on them. On the other hand, the main point of this section is the introduction of a simplified scheme which is still able to highlight the important features of our study with a much more realistic physical setup.

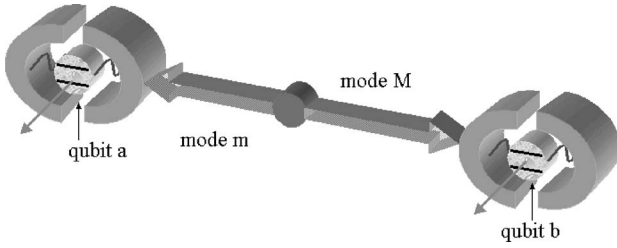


FIG. 6. Scheme of principle of the experimental to be realized in order to test the entangling power as described in Sec. III. Modes m and M are assumed to be addressing two cavities through which two independent qubits pass. The cavity-qubit interaction changes the refraction index of the cavity, allowing for the feeding by the external fields.

The idea is depicted in Fig. 7 where the most striking difference with respect to the previous configuration is the presence of a single cavity and no traveling light field. Indeed, it is well known [40] (see also Paternostro *et al.* [20]) that the dispersive interaction between a single two-level system and a cavity mode would lead to an effective Hamiltonian reading

$$\hat{H}_{mM}^{\text{eff}} = \chi \hat{M}^\dagger \hat{M} |1_a\rangle\langle 1|, \quad (12)$$

where the microscopic subsystem m has been identified with the qubit a whose spectrum has been rescaled so that its ground state has zero energy. We have indicated $\chi = \Omega^2/\delta$ with $\delta \gg \Omega$ the large atom-field detuning. This model can be achieved by assuming a qubit one-cavity mode JC interaction in the presence of a static electric field. The induced Stark shift on the atomic levels creates a detuning δ such that Eq. (12) holds. The propagator generated by this Hamiltonian, starting from the state $|+\rangle_a \otimes \rho_M^{\text{th}}(V, d) = (1/\sqrt{2})(|0\rangle + |1\rangle)_a \otimes \rho_M^{\text{th}}(V, d)$, creates a generalized catlike state between a thermal displaced state of the cavity field mode and a two-level atom. The displacement of the thermal field can be effectively performed via the modification to the cavity refractive index induced by the presence of the two-level atom. This acts as an effective nonlinear intracavity medium which shifts the resonance frequency of the cavity and can inject an external coherent state of its amplitude β . The effective displacement would result in $d = \beta \Delta t$ with Δt the time-of-flight for atom a crossing the cavity [41].

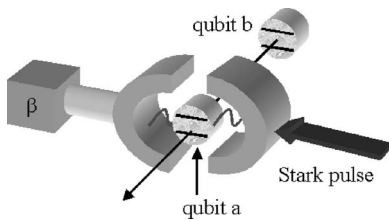


FIG. 7. Scheme for the experimental verification of the analysis presented in this paper. The scheme reproduces the single-qubit transfer protocol we address in the body of the paper. In this case, the generalized catlike state is given by the state of qubit a and the cavity mode field. Qubit b is ancillary and is used just in order to test the entangling power in a less demanding way.

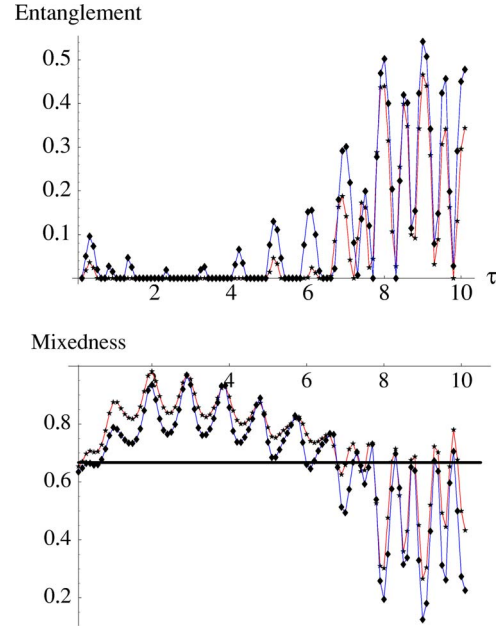


FIG. 8. (Color online) (a) Entangling power of the state $\int d^2 P_M^{\text{th}}(V, d) \rho_\psi(\tau)$ against τ for $V=10$ and $d=10$ (\blacklozenge) and $V=10$ with $d=7$ (\star). (b) Mixedness of the same state as a function of the rescaled interaction time. The mixedness threshold for teleportation is also shown (straight line).

We are thus considering a hybrid catlike state where the CV and the qubit parts have clearly distinguished physical embodiments. As soon as qubit a leaves the cavity, a second qubit b , identical to the first, crosses the cavity in absence of the Stark electric field (i.e., the interaction model is the standard JC one). By interacting with the cavity field, this process leads to an entangled state of subsystems a , M , and b . Tracing out the cavity field, we are left with a reduced two-qubit state whose entanglement represents, again, a sufficient condition for the entanglement in the generalized catlike state. We are thus describing a unilateral entanglement-transfer process for a modified entangling power test [42].

Obviously, the quantitative analysis reported in Sec. III are not applicable to the present modified protocol and the effectiveness of the entanglement transfer process should be retested. However, this is a straightforward process which may be derived directly from what is presented in Eqs. (9) and (10). We find that the structure of the reduced density matrix $\rho_{\psi,ab} = \text{Tr}_M(\hat{U}_{Mb} \hat{U}_{mM}^{\text{eff}} \rho_M^{\text{th}} \otimes |+\rangle_a \langle +| \otimes |g\rangle_b \langle g| \hat{U}_{mM}^{\text{eff} \dagger} \hat{U}_{Mb}^\dagger)$ is similar to Eq. (9). The calculation of the negativity of partial transposition gives us, once again, useful information about the entanglement within this two-qubit state, transferred after the M - b interaction. The results are shown in Fig. 8(a) for the same parameters as in Fig. 3. At the same time, in Fig. 8(b) we reprise our teleportation example and present the analysis in terms of linearized entropy. It is evident that a good degree of entanglement can still be found (despite the high peaks of Fig. 3 have disappeared), with a quite low degree of mixedness of the associated quantum channel also for this modified entangling test protocol. Obviously, this represents a huge advantage in terms of experimental feasibility as all the ingredients for the entangling power test are

within the current state of the art. Considerations analogous to those made about the symmetric entangling power test in Sec. III can be adapted to the case here at hand. From an experimental point of view, resolving the oscillations of the entanglement function against time could be challenging. The zones of large entanglement and purity (i.e., small mixedness) correspond to a maximum transfer of quantum correlations from the entangler to the receivers and a partial disentanglement of these two subsystems. Therefore, the time-averaged entanglement could gain some practical relevance in estimating, roughly, the entanglement content of the two-qubit state after the asymmetric entanglement transfer process. For the curves plotted in Fig. 8, such a quantity can be as large as 0.25, in the significant range of interaction times which includes the region of faster oscillations.

V. REMARKS

In investigating the entangled properties of mesoscopic systems at finite temperature, in the quantum optics domain, we often face some difficulties related to a certain lack of analytical tools. This has strongly limited the insight we could gain about the specific behavior, in terms of quantum correlations, of particular classes of states (especially non-Gaussian states).

These difficulties have forced the researchers to look for ways to bypass the problem and infer the quantumness of a state. It appears that such the alternative tests are based on the restriction of the analysis from infinite to finite dimensional Hilbert spaces. This can be done by effective (formal) projection of a CV state onto bipartite Hilbert sectors (as done in Refs. [10,13]) as well as looking at the amount of nonclassical correlations that a given state under investigation can transfer to mutually noninteracting qubits [22]. In this paper we have performed some interesting steps along these directions, investigating the entanglement properties of a class of recently introduced (highly non-Gaussian) generalized catlike states [16]. Our approach has been twofold. In the first place, we have calculated the entanglement of the catlike state by partitioning the Hilbert space of the combined system into manifolds spanned by the states of an effective bipartite two-level system. The entanglement of the whole state, then, is the result of a thermal average of the quantum correlations within each manifold. The qualitative features highlighted by this approach have been confirmed, in the second place, by testing the entangling power of the generalized catlike state with respect to two initially separable qubits. This second approach is particularly useful under a practical as well as a theoretical viewpoint. It has revealed that powerful experimental criteria exist, for the entanglement investigation, beyond the CV criteria for inseparability [21]. Our study is, thus, a particularly illuminating case of this second, more operative scenario.

As an additional example of the effectiveness of the entangling power test, here we briefly assess the problem of the entanglement in the class of states generated by the entire protocol described by the setup in Fig. 1 (dashed-box included). The detection of mode m is performed onto the basis $\{|+\rangle, |-\rangle\}$ [with $|-\rangle = (1/\sqrt{2})(|0\rangle - |1\rangle)$]. Conditioned on finding $|\pm\rangle_m$, the action of the beam splitter which mixes mode M to vacuum gives rise to the state (we assume $\varphi = \pi$)

$$\rho^\pm = \mathcal{N}^\pm \int d^2\alpha P^{th}(V, d) \{ |\sigma, -\sigma\rangle\langle\sigma, -\sigma| + |\sigma, -\sigma\rangle\langle-\sigma, \sigma| \pm |-\sigma, \sigma\rangle\langle\sigma, -\sigma| \pm |-\sigma, \sigma\rangle\langle-\sigma, \sigma| \}, \tag{13}$$

where $\sigma = \alpha/\sqrt{2}$ and \mathcal{N}^\pm are proper normalization factors. In order to fix the ideas, let us focus on the case of $|+\rangle_m$ being found with $d=0$, for which the expression of the variance matrix is particularly straightforward, reading

$$\gamma^+ = \begin{pmatrix} \frac{V^2+1}{2V} & 0 & -\frac{(V-1)^2}{2V} & 0 \\ 0 & \frac{V^2+1}{2V} & 0 & -\frac{(V-1)^2}{2V} \\ -\frac{(V-1)^2}{2V} & 0 & \frac{V^2+1}{2V} & 0 \\ 0 & -\frac{(V-1)^2}{2V} & 0 & \frac{V^2+1}{2V} \end{pmatrix}. \tag{14}$$

It is easy to check that Simon’s separability condition is not violated by Eq. (13) so that no firm statement about the entanglement properties of this state can be made. However, following the lines depicted in Ref. [16], it is straightforward to show that Eq. (13) violates a Bell-CHSH inequality [43] regardless of V and d , thus revealing an inherent quantum entanglement of the state. This result is confirmed by the application of the entangling power test which shows that entanglement (as large as ≈ 0.6 for V around 50 and $d=5$) can be transferred to two mutually noninteracting qubits using the symmetric scheme of Sec. III. This second example completes and complements our investigation which, we believe, represents an interesting example of the possibilities of revealing quantum nonlocality in nontrivial situations of mesoscopic superpositions at high temperature.

ACKNOWLEDGMENTS

We acknowledge useful discussions with Professor P. L. Knight and Dr. J. Fiurášek and communication with A. Ferreira. This work has been supported by The Leverhulme Trust (Grant No. ECF/40157), the Australian Research Council, the UK EPSRC, and the Korea Research Foundation (Grant No. 2003-070-C00024).

- [1] D. Deutsch, Proc. R. Soc. London, Ser. A **400**, 97 (1985); D. Gottesman and I. L. Chuang, Nature (London) **402**, 390 (1999); J. Eisert, K. Jacobs, P. Papadopoulos, and M. B. Plenio, Phys. Rev. A **62**, 052317 (2000).
- [2] H.-J. Briegel, W. Dur, J. I. Cirac, and P. Zoller, Phys. Rev. Lett. **81**, 5932 (1998); L.-M. Duan, M. D. Lukin, J. I. Cirac, and P. Zoller, Nature (London) **414**, 413 (2001).
- [3] R. Raussendorf and H. J. Briegel, Phys. Rev. Lett. **86**, 5188 (2001); R. Raussendorf, D. E. Browne, and H. J. Briegel, Phys. Rev. A **68**, 022312 (2003), and references within.
- [4] J. Eisert, M. Wilkens, and M. Lewenstein, Phys. Rev. Lett. **83**, 3077 (1999); L. Vaidman, Y. Aharonov, and D. Z. Albert, *ibid.* **58**, 1385 (1987); M. Paternostro, M. S. Tame, and M. S. Kim, New J. Phys. **7**, 226 (2005).
- [5] C. Brukner, V. Vedral, and A. Zeilinger, e-print quant-ph/0410138; C. Lunkes, C. Brukner, and V. Vedral, Phys. Rev. Lett. **95**, 030503 (2005).
- [6] V. Vedral, New J. Phys. **6**, 102 (2004).
- [7] R. Filip, M. Dusek, J. Fiurášek, and L. Mišta, Phys. Rev. A **65**, 043802 (2002).
- [8] S. Bose, K. Jacobs, and P. L. Knight, Phys. Rev. A **56**, 4175 (1997).
- [9] S. Mancini, V. Giovannetti, D. Vitali, and P. Tombesi, Phys. Rev. Lett. **88**, 120401 (2002).
- [10] A. Ferreira, A. Guerreiro, and V. Vedral, e-print quant-ph/0504186.
- [11] G. S. Agarwal and A. Biswas, New J. Phys. **7**, 211 (2005).
- [12] M. Hillery and M. S. Zubairy, e-print quant-ph/0507168.
- [13] S. Bose, I. Fuentes-Guridi, P. L. Knight, and V. Vedral, Phys. Rev. Lett. **87**, 050401 (2001).
- [14] C. Brukner, M. S. Kim, J.-W. Pan, and A. Zeilinger, Phys. Rev. A **68**, 062105 (2003).
- [15] A. Peres, Phys. Rev. Lett. **77**, 1413 (1996); M. Horodecki, P. Horodecki, and R. Horodecki, Phys. Lett. A **223**, 1 (1996); J. Lee, M. S. Kim, Y. J. Park, and S. Lee, J. Mod. Opt. **47**, 2151 (2000).
- [16] H. Jeong and T. C. Ralph, e-print quant-ph/0410210.
- [17] E. Schrödinger, Naturwiss. **23**, 807 (1935).
- [18] C. Monroe, D. M. Meekhof, B. E. King, and D. J. Wineland, Science **272**, 1131 (1996).
- [19] B. C. Sanders, Phys. Rev. A **45**, 6811 (1992).
- [20] S. J. van Enk and O. Hirota, Phys. Rev. A **64**, 022313 (2001); H. Jeong, M. S. Kim, and J. Lee, *ibid.* **64**, 052308 (2001); X. Wang, *ibid.* **64**, 022302 (2001); T. C. Ralph, W. J. Munro, and G. J. Milburn, Proc. SPIE **4917**, 1 (2002); H. Jeong and M. S. Kim, Phys. Rev. A **65**, 042305 (2002); T. C. Ralph, A. Gilchrist, G. J. Milburn, W. J. Munro, and S. Glancy, *ibid.* **68**, 042319 (2003); N. B. An, *ibid.* **68**, 022321 (2003); M. Paternostro, M. S. Kim, and P. L. Knight, *ibid.* **71**, 022311 (2004).
- [21] R. Simon, Phys. Rev. Lett. **84**, 2726 (2000).
- [22] M. Paternostro, W. Son, M. S. Kim, G. Falci, and G. M. Palma, Phys. Rev. A **70**, 022320 (2004).
- [23] M. S. Kim, J. Lee, and W. J. Munro, Phys. Rev. A **66**, 030301(R) (2002).
- [24] L.-M. Duan, G. Giedke, J. I. Cirac, and P. Zoller, Phys. Rev. Lett. **84**, 2722 (2000).
- [25] D. Wilson, J. Lee, and M. S. Kim, J. Mod. Opt. **50**, 1809 (2002).
- [26] A. Peres, Phys. Rev. Lett. **77**, 1413 (1996); M. Horodecki, P. Horodecki, and R. Horodecki, Phys. Lett. A **223**, 1 (1996); J. Lee, M. S. Kim, Y. J. Park, and S. Lee, J. Mod. Opt. **47**, 2151 (2000).
- [27] M. Paternostro, G. Falci, M. Kim, and G. M. Palma, Phys. Rev. B **69**, 214502 (2004); I. Wilson-Rae and A. Imamoglu, *ibid.* **65**, 235311 (2002); F. Marquardt and C. Bruder, *ibid.* **63**, 054514 (2001); J. M. Taylor, G. Giedke, H. Christ, B. Paredes, J. I. Cirac, P. Zoller, M. D. Lukin, and A. Imamoglu, e-print cond-mat/0407640.
- [28] Properly arranged matter-light interactions, in the regime of electromagnetically induced transparency, can produce a cross-phase modulation with huge nonlinear rates [see M. Paternostro, M. S. Kim, and B. S. Ham, Phys. Rev. A **67**, 023811 (2003) for a protocol which generates entangled coherent states]. However, as far as the authors are concerned, there has not been a satisfactory experimental implementation yet.
- [29] This argument can be pictorially understood by geometrical considerations in the phase-space analogous to those done, for instance, in Ref. [31].
- [30] J. Fiurášek, L. Mišta, Jr., and R. Filip, Phys. Rev. A **67**, 022304 (2003); H. Jeong, Ph.D. thesis, Queen's University Belfast, U.K., 2003; S. D. Barrett, P. Kok, K. Nemoto, R. G. Beausoleil, W. J. Munro, and T. P. Spiller, Phys. Rev. A **71**, 060302(R) (2005); K. Nemoto and W. J. Munro, Phys. Rev. Lett. **93**, 250502 (2004).
- [31] H. Jeong, Phys. Rev. A **72**, 034305 (2005). In this reference, it has been numerically shown that, under proper conditions, decoherence may be overcome in optical fibers with small nonlinearities for generation of macroscopic entanglement.
- [32] M. C. Arnesen, S. Bose, and V. Vedral, Phys. Rev. Lett. **87**, 017901 (2001).
- [33] J. Eisert, K. Jacobs, P. Papadopoulos, and M. B. Plenio, Phys. Rev. A **62**, 052317 (2000); D. Collins, N. Linden, and S. Popescu, *ibid.* **64**, 032302 (2001); M. Paternostro, M. S. Kim, and G. M. Palma, J. Mod. Opt. **50**, 2075 (2003).
- [34] M. Paternostro, W. Son, and M. S. Kim, Phys. Rev. Lett. **92**, 197901 (2004); B. Kraus and J. I. Cirac, *ibid.* **92**, 013602 (2004); M. Paternostro, M. S. Kim, and W. Son, Int. J. Quantum Inf. **3**, 213 (2005).
- [35] C. A. Sackett, D. Kielpinski, B. E. King, C. Langer, V. Meyer, C. J. Myatt, M. Rowe, Q. A. Turchette, W. M. Itano, and D. J. Wineland, Nature (London) **404**, 256 (2000).
- [36] G. Toth and O. Guhne, Phys. Rev. Lett. **94**, 060501 (2005).
- [37] Some advantages, in looking for an analytical expression for the eigenvalues come from the fact that, for $\varphi = \pi$, $G_1 = -H_1$, and $G_2 = -F_2$, which considerably simplify the expression of $\int d^2 P_M^{\text{th}}(V, d) \rho_{\psi}(\tau)$.
- [38] S. Bose and V. Vedral, Phys. Rev. A **61**, 040101(R) (2000).
- [39] J. Lee, M. Paternostro, M. S. Kim, and S. Bose, e-print quant-ph/0509095.
- [40] B.-G. Englert, N. Sterpi, and H. Walther, Opt. Commun. **100**, 526 (1993); L. G. Lutterbach and L. Davidovich, Phys. Rev. Lett. **78**, 2547 (1997); M. S. Kim and J. Lee, Phys. Rev. A **61**, 042102 (2000).
- [41] L. Davidovich, M. Brune, J. M. Raimond, and S. Haroche, Phys. Rev. A **53**, 1295 (1996).
- [42] The process may also be seen as a variant of the entanglement-swapping protocol.
- [43] J. S. Bell, Physics (Long Island City, N.Y.) **1**, 195 (1964); J. F. Clauser *et al.*, Phys. Rev. Lett. **23**, 880 (1969).